CHIN. PHYS. LETT. Vol. 36, No. 7 (2019) 078301

Mechanism for the Self-Assembly of Hollow Micelles from Rod-Coil Block Copolymers

Lingyun Zhang(张凌云)**

Beijing National Laboratory for Condensed Matter Physics, Institute of Physics, Chinese Academy of Sciences, Beijing 100190

(Received 16 April 2019)

The mechanism for the self-assembly of hollow micelles from rod-coil diblock copolymers is proposed. In a coil-selective solvent, the diblock copolymers self-assemble into a layered structure. It is assumed that the rigid rods form an elastic shell whose properties are dictated by a bending energy. For a hollow micelle, the coils outside the micelle form a brush, while the coils inside the micelle can be in two different states, a brush or an adsorption layer, corresponding to symmetric or asymmetric configurations, respectively. The total energy density of a hollow micelle is calculated by combining the interfacial energy, elastic bending energy and the stretching energy of the brushes. For the asymmetric configuration with a polymer brush on one side, the competition between the elastic bending energy and the brush stretching energy leads to a finite spontaneous curvature, stabilizing hollow spherical micelles. Comparison of the free energy density for different geometries demonstrates that transitions for the different geometry micelles are controlled by the degree of polymerization of the coils and the length of the rods. These results are in agreement with the experimental results.

PACS: 83.10.Tv, 61.82.Pv, 82.35.Jk DOI: 10.1088/0256-307X/36/7/078301

Synthetic hollow spherical structures in the different materials have attracted much interest and attention because this kind of system has several potential applications in many fields such as optoelectronics and nanotechnologies.[1–6] The selectivity condition thermodynamically prefers one of the two blocks so that the self-assembly structures can be achieved by controlling solvent.[7–12] Jenekehe and Chen used the rod-coil diblock copolymer to observe the self-assembly in a selective solvent into the hollow spherical micelles.[13] The experimental aim is to illustrate that the ordered microporous materials can be self-assembly formed into long range crystalline order with spherical, cylindrical and lamellar structures. The experimental system about the rod-coil diblock copolymer is PPQ_mPS_n in carbon disulfide, which is a selective solvent for PS block.

The experimental results stimulate us to establish the model and set up the theory to explore the form mechanism of hollow spherical micelles and explain these experimental phenomena. In this Letter, we calculate the free energy for the rod-coil block copolymer, which forms a few kinds of polymer brushes, flat, sphere, cylinder. Three free energy terms have been considered, the interfacial energy, bending elastic energy and brush energy. For a hollow micelle, the coils outside the micelle form a brush, while the coils inside the micelle can be in two different states, a brush or an adsorption layer, corresponding to symmetric or asymmetric configurations respectively. Comparison of the free energy density for different geometries in the asymmetric configuration demonstrates that transition from lamellar to cylindrical to spherical micelles is controlled by the degree of polymerization of the coils and the length of the rods.

For hollow micelle, the coils outside the micelle form a brush, while the coils inside the micelle can be in two different states, a brush or an adsorption layer, corresponding to symmetric or asymmetric configuration. The single sphere is shown in Fig. 1, and the solvent is inside and outside of sphere. Our basic idea is that the coil is like the brush, its height outside of sphere is h_o and inside is h_i. The rods are considered as a continuous system, and form the elastic shell, its thickness is d. The stretched coils made up the lateral force, therefore, it is the competition between the packing energy and binding energy that result in the structural formation.

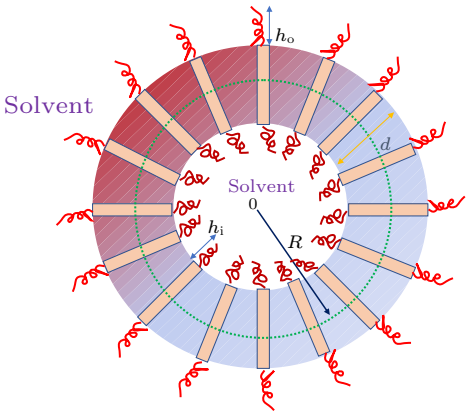

Fig. 1. Schematic illustration of the self-assembly of hollow micelles from rod-coil block copolymers. The rigid rods are formed in an elastic shell. For a hollow micelle, the coils outside the micelle form a brush, while the coils inside the micelle are in two different states. Symmetric configuration: the coils inside the micelle is also a brush, where h_o and h_i are the heights of coils outside and inside of micelle, respectively, d is the length of rod, and R is the average radius of shell.

**Corresponding author. Email: lyzhang@iphy.ac.cn

© 2019 Chinese Physical Society and IOP Publishing Ltd

The total surface at R is

$$S_p(R) = \frac{2\pi^{p/2}}{\Gamma(p/2)} R^{p-1} L^{3-p}, \tag{1}$$

where $p = 1$, 2 and 3 denotes the lamellar, cylindrical and spherical, respectively, $\Gamma(p/2)$ is the Gamma function $\Gamma(\alpha) = \int_0^\infty x^{\alpha-1} e^{-x} dx$, its properties include $\Gamma(\alpha+1) = \alpha\Gamma(\alpha)$, $\Gamma(1/2) = \sqrt{\pi}$ and $\Gamma(1) = 1$.

The total volume at R is

$$V_p(R) = \frac{2\pi^{p/2}}{p\Gamma(p/2)} R^p L^{3-p}. \tag{2}$$

Therefore, the area and volume of the cell are

$$\begin{aligned} S_p &= C_p R^{p-1}, \\ V_p &= \frac{C_p}{p} R^p, \end{aligned} \tag{3}$$

where $C_p = \frac{2\pi^{p/2}}{\Gamma(p/2)} L^{3-p}$.

We consider that the brushes are grafted in the surface of R and the height of the brush is h. If the area per chain is Σ, the total number of chains is

$$n = S_p/\Sigma. \tag{4}$$

The value of N is defined as the degrees of polymerization, then the filled volume is $V_\mathrm{f} = nN$, i.e.,

$$V_\mathrm{f} = \frac{S_p N}{\Sigma} = \sigma S_p N, \tag{5}$$

where $\sigma = 1/\Sigma$ stands for the chains per unit area. Under the incompressibility condition

$$V_p(R+h) = V_p(R) + V_\mathrm{f}, \tag{6}$$

the heights of brushes grafted outside of the interface can be expressed as

$$\frac{h_\mathrm{o}}{R} = \left(1 + \frac{pN\sigma}{R}\right)^{\frac{1}{p}} - 1. \tag{7}$$

If the brushes are grafted inside of the interface, $V_p(R) = V_p(R-h) + V_\mathrm{f}$

$$\frac{h_\mathrm{i}}{R} = 1 - \left(1 - \frac{pN\sigma}{R}\right)^{\frac{1}{p}}. \tag{8}$$

It is assumed that the free end of the polymer brush lies at the distance r_0 from the surface of the micelle. The chain lies along the radius of the micelle and hence is characterized by the scalar function $r(n)$, which is the distance from the surface $r(N) = r_0$.

The local extension of the chain is defined as $E(r, r_0) = \frac{dr}{dn}$. The total number of monomers in one chain can be expressed as

$$N = \int_0^N dn = \int_0^{r_0} \frac{dr}{E(r, r_0)}. \tag{9}$$

If $g(r_0)dr_0$ is defined as the number of chains whose ends lie in the interval dr_0, then we have

$$Q = \int_0^R g(r_0) dr_0, \tag{10}$$

which is the number of chains forming the micelle, and

$$\int_r^R \frac{g(r_0)}{E(r, r_0)} dr_0 = S_p(R - r). \tag{11}$$

In terms of Refs. [14-16], the free energy of the polymer brush can be written as

$$U_r = \frac{Q}{4a^2} \int_0^\infty \left(\frac{dr}{dn}\right)^2 dn. \tag{12}$$

Using $dr = Edn$ and $a = 1$

$$U_r^p = \frac{1}{4} \int_0^h dr_0 \int_0^{r_0} dr E(r, r_0) g_p(r_0). \tag{13}$$

Based on $E(r, r_0) = \frac{\pi}{2N}(r_0^2 - r^2)^{1/2}$, one finds

$$\frac{2N}{\pi} \int_r^h \frac{g(r_0)}{(r_0^2 - r^2)^{1/2}} = C_p (R - r)^{p-1}. \tag{14}$$

Let $t = (r_0/h)^2$ and $u = (r/h)^2$,

$$\int_u^1 \frac{f_p(t)}{\sqrt{t-u}} dt = \frac{2\pi^{p/2}}{\Gamma(p/2)} \left(\frac{R}{h} - u^{1/2}\right)^{p-1}, \tag{15}$$

where

$$f_p\left(\frac{{r_0}^2}{h^2}\right) = \frac{N}{\pi} \frac{h}{r_0} \frac{1}{h^{p-1}} g_p(r_0), \tag{16}$$

then

$$\begin{aligned} &\int_u^1 \frac{f_1(t)}{\sqrt{t-u}} dt = 2, \\ &\int_u^1 \frac{f_2(t)}{\sqrt{t-u}} dt = 2\pi \left(\frac{R}{h} - u^{1/2}\right), \\ &\int_u^1 \frac{f_3(t)}{\sqrt{t-u}} dt = 4\pi \left(\frac{R^2}{h^2} - 2\frac{R}{h} u^{1/2} + u\right). \end{aligned} \tag{17}$$

We need to carry out

$$\int_u^1 \frac{h_n(t)}{\sqrt{t-u}} dt = u^{n/2}, \tag{18}$$

where $n = 0$, 1 and 2. Using $x = 1 - t$ and $v = 1 - u$, we have

$$\int_0^v \frac{h_n(x)}{\sqrt{v-x}} dx = (1-v)^{n/2}. \tag{19}$$

Dividing both sides by $\sqrt{s-v}$ and integrating for v,

$$h_n(x) = \frac{\partial q_n(x)}{\partial x}, \tag{20}$$

where

$$q_n(x) = \frac{1}{\pi} \int_0^x dv \frac{(1-v)^{n/2}}{\sqrt{x-v}}. \tag{21}$$

The integral results of q_n for $n = 1$, 2 and 3 can be obtained as follows:

$$\begin{aligned} q_0(x) &= \frac{1}{\pi}\int_0^x \frac{dv}{\sqrt{(x-v)}} = \frac{2}{\pi}x^{1/2}, \\ q_1(x) &= \frac{1}{\pi}\int_0^x \frac{\sqrt{1-v}}{\sqrt{x-v}}dv \\ &= \frac{2}{\pi}\Big[x^{1/2} + \frac{1}{2}(1-x)\ln\frac{1+x^{1/2}}{1-x^{1/2}}\Big], \\ q_2(x) &= \frac{1}{\pi}\int_0^x dv\frac{1-v}{\sqrt{x-v}} \\ &= \frac{2}{\pi}\Big(x^{1/2} - \frac{2}{3}x^{3/2}\Big). \end{aligned} \tag{22}$$

The stretching energy of the polymer brush is

$$U_r^p = f_0\frac{h^3}{N^2}S_p(R)l_p\Big(\frac{h}{R}\Big), \tag{23}$$

where $f_0 = \pi^2/48$, and $l_p(x)$ are

$$\begin{aligned} l_1(x) &= 1, \\ l_2(x) &= 1 - \frac{3}{4}x, \\ l_3(x) &= 1 - \frac{3}{2}x + \frac{3}{5}x^2. \end{aligned} \tag{24}$$

The interfacial energy is generally expressed as

$$F_{\rm i}^p = \gamma S_p(R) = \gamma C_p R^{p-1}, \tag{25}$$

where γ is the interfacial tension.

The bending energy per unit area generally reads

$$f_{\rm b} = \frac{\kappa}{2}H^2, \tag{26}$$

where κ is the elastic modulus, and H is the mean curvature $H = (c_1 + c_2)/2$ with c_1 and c_2 being the maximum and minimum curvature values.

For a flat layer, $C_1 = \frac{1}{R_1} = 0$ and $C_2 = \frac{1}{R_2} = 0$, i.e., $H = 0$. Thus the bending energy density of the flat plane is zero,

$$f_{\rm b}^{\rm f} = 0. \tag{27}$$

For a cylinder (or the hexagonal phase), $C_1 = \frac{1}{R_1} = \frac{1}{R}$ and $C_2 = \frac{1}{R_2} = 0$, which rises to $H = \pm\frac{1}{2R}$ ($-1/2$ in the case of an inverse hexagonal phase), then

$$f_{\rm b}^{\rm c} = \frac{\kappa}{8R^2}. \tag{28}$$

For a sphere/micelle, $C_1 = \frac{1}{R_1} = \frac{1}{R}$ and $C_2 = \frac{1}{R_2} = \frac{1}{R}$, which results in $H = \pm\frac{1}{R}$, then

$$f_{\rm b}^{\rm s} = \frac{\kappa}{2R^2}. \tag{29}$$

Therefore, the elastic bending energy is

$$F_{\rm b}^p = \frac{a_p\kappa}{R^2}S_p(R), \tag{30}$$

where a_p is a dimensional parameter, which are 0, 0.125 and 0.5 for the flat, cylinder and sphere, respectively.

On the other hand, κ depends on the bilayer thickness $\kappa = Kd^2$,[17] then

$$F_{\rm b}^p = \frac{a_pKd^2}{R^2}S_p(R). \tag{31}$$

In a word, we can obtain the total free energy density of the rod-coil polymer, which sum up the interfacial, elastic bending and brush energy,

$$f_p = \frac{F_p}{S_p(R)} = \gamma + \frac{a_pKd^2}{R^2} + f_0\frac{h^3}{N^2}l_p\Big(\frac{h}{R}\Big), \tag{32}$$

where x is defined as the ratio of brush numbers between the inside and outside of surface $x = \frac{n_{\rm in}}{n}$. Therefore, we have $n_{\rm in} = xn$ and $n_{\rm out} = (1-x)n$. Furthermore, the densities outside of surface and inside of surface are respectively $\sigma_{\rm out} = (1-x)\sigma_0$ and $\sigma_{\rm in} = x\sigma_0$. On the other hand, the difference of free energy density among the sphere, cylinder and flat can be defined as

$$\Delta f^p = f_p - f_1. \tag{33}$$

We choose the flat as a reference plane, which is the symmetry plane for brushes, i.e., $x = 1/2$, under this condition, $N_{\rm out} = N_{\rm in} = N$ and $\sigma_{\rm out} = \sigma_{\rm in} = \sigma_0/2$. Furthermore, $h_{\rm o} = \sigma_{\rm out}N = \sigma_{\rm in}N = h_{\rm i} = \frac{\sigma_0 N}{2}$, thus

$$f_1 = \gamma + \frac{f_0}{4}N\sigma_0^3. \tag{34}$$

Let $R_{\rm c} = \frac{R_{\rm q}}{R}$, where $R_{\rm q} = 2(1-x)N\sigma_0$. The free energy densities of cylinder and sphere are

$$\begin{aligned} \frac{\Delta f^2}{\varepsilon_0} &= \alpha R_{\rm c}^2 + \frac{\beta}{R_{\rm c}^3}[(1+R_{\rm c})^{1/2} - 1]^3[1 \\ &\quad + 3(1+R_{\rm c})^{1/2}] - 1, \\ \frac{\Delta f^3}{\varepsilon_0} &= 4\alpha R_{\rm c}^2 + \frac{2\beta}{R_{\rm c}^3}\Big[\Big(1+\frac{3}{2}R_{\rm c}\Big)^{1/3} - 1\Big]^3 \\ &\quad \cdot\Big\{-1 + 3\Big(1+\frac{3}{2}R_{\rm c}\Big)^{1/3} + \frac{6}{5}\Big[\Big(1 \\ &\quad + \frac{3}{2}R_{\rm c}\Big)^{1/3} - 1\Big]^2\Big\} - 1, \end{aligned} \tag{35}$$

where some parameters are

$$\begin{aligned} \varepsilon_0 &= \frac{f_0}{4}N\sigma_0^3, \\ \varepsilon_{\rm f} &= \frac{f_0R_{\rm q}^3}{4N^2} = 2f_0(1-x)^3\,N\sigma_0^3, \\ \varepsilon_d &= \frac{Kd^2}{8R_{\rm q}^2} = \frac{Kd^2}{32(1-x)^2N^2\sigma_0^2}, \\ \alpha &= \frac{\varepsilon_d}{\varepsilon_0} = \frac{Kd^2}{8f_0(1-x)^2N^3\sigma_0^5}, \\ \beta &= \frac{\varepsilon_{\rm f}}{\varepsilon_0} = 8(1-x)^3. \end{aligned} \tag{36}$$

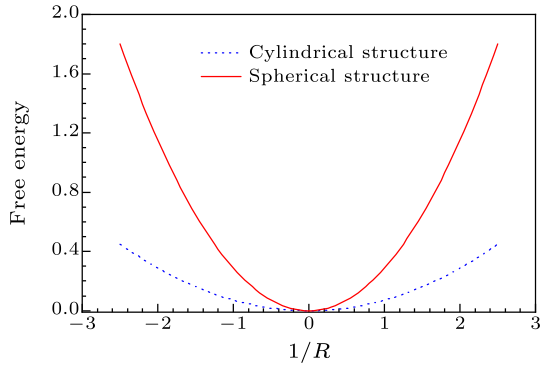

Fig. 2. Variation of the free energy as a function of the inverse of shell radius R. The flat is a reference value. Solid line represents the spherical structure, and dotted line denotes the cylindrical structure.

For symmetric configuration as shown in Fig. 1, the free energy density of flat can be chosen as zero because the flat is a reference value. We calculate the free energy densities for sphere and cylinder respectively. Numerical results are plotted in Fig. 2, where the free energy density is demonstrated as a function of the inverse of shell radius R. The solid line denotes the relation between the free energy density and $1/R$ of the spherical structure, and the dotted line is the relation between the free energy density and $1/R$ of the cylindrical structure. Among the three structures, the most stable structure is flat because it has the lowest energy. This result tells us that there is no hollow spherical structure in the symmetric configuration.

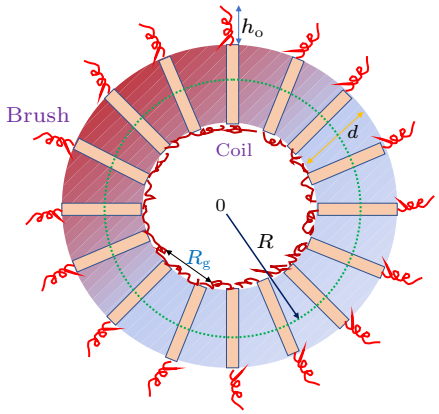

Fig. 3. Asymmetric configuration: most of the coils are outside of surface and the coils inside the micelle is an adsorption layer, where R_g is the gyration radius.

The asymmetric configuration is shown in Fig. 3, most of the brushes are outside of surface, and the brush inside of surface is almost zero. In this case, the coils inside surface is like to form an adsorption layer, where x is a fixed number. Next, we will give a comparison of free energy for the different geometry configurations, i.e., the free energy density of the different configures is a function of $\frac{1}{R}$, which is varied with the difference of α.

It is shown that the relation between the free energy density and $1/R$ of cylindrical structure for different values of α in Fig. 4(a). The dotted line describes $\alpha = 0.05$, the dashed line denotes $\alpha = 0.01$, and the solid line is $\alpha = 0.0001$. The theoretical calculations indicate that the free energy is the lowest at $\alpha = 0.0001$ for the cylindrical structure. In other words, the cylindrical structure will be approached to the stable state with the decrease of α. For the spherical structure, Fig. 4(b) illustrates the free energy and the inverse of shell radius R for different α. The solid line is $\alpha = 0.0001$, the dashed line denotes $\alpha = 0.0005$, and the dotted line is $\alpha = 0.01$. As the parameter α decreases, the spherical phase behavior will give rise to the stable state. It is illustrated that the smaller α exhibits a behavior of stable hollow spheres.

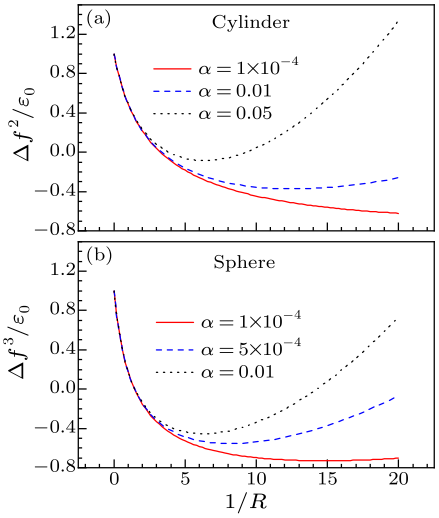

Fig. 4. (a) The theoretical calculation of cylindrical structure for the function of the free energy as the inverse of shell radius R in the three different α parameters. (b) The free energy as a function of the inverse of R in the spherical phase for α parameters at $\alpha = 0.01$, $\alpha = 0.0005$ and $\alpha = 0.0001$.

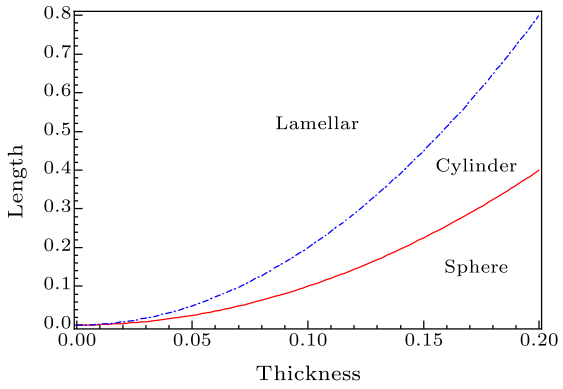

Fig. 5. As shown in the phase diagram for selective solvent, there are three zones of phase equilibrium. From bottom to top, the first zone is the spherical phase, the second zone is the cylindrical phase, and the third zone is the lamellar phase. The dashed line denotes the transition from L phase to C phase, and the solid line represents the transition from C phase to S phase. The degree of polymerization of coils is a function of the rod thickness for the different geometric configurations.

The most interesting phenomenon is the structural phase transition. As shown in Fig. 5, three phases have

been produced, which are sphere, cylinder and lamellar. From bottom to top, the first zone is the spherical phase, the second zone is the cylindrical phase, and the third zone is the lamellar phase. The dashed line denotes the transition from L phase to C phase, and the solid line represents the transition from C phase to S phase. The theoretical phase diagram in the selective solvent demonstrates that the spherical structure is a stable state and reveals the mechanism of hollow spheres in the experimental observation. Because α is dependent on the degree of polymerization of the coils N and the length of the rods d, we can find that the increasing N and decreasing d lead into phase transition among lamellar, cylinder and sphere. In a certain range, the free energy of spherical structure has the minimum value. The theoretical results explain the experimental phenomena in the results of Ref. [13]. Therefore, we can give a reason why the hollow sphere can be formed. Its physics mechanism results from the symmetry break in the different numbers of brush between the inside and outside of shell. Meanwhile, the competition between packing energy and bending energy results in a finite spontaneous curvature.

The dynamics investigation for constructing phase diagrams of polymers is of significant importance for a thorough understanding of structural transitions in various kinds of polymers.[18] However, the method here for finding the minimum values of free energy for different micellar structures is employed to construct phase diagrams. The micellar system consists of rod-coil copolymer and solvent. The thermodynamics condition of solvent with selectivity preferring one of the two blocks produces diversified structures.[19] The effect of solvent on the hollow micelle results in our theoretical model with the formation of two different states.

In summary, we have developed a theoretical model with different geometric configurations to illustrate the self assembly mechanism of hollow micelles from rod-coil copolymers. The strong stretching in brushes has been applied to obtain the free energy of coils. We calculate the free energy including elastic bending energy, interfacial energy and stretching energy to find the phase behaviors in selective solvents. The parameters depend on the degree of polymerization of coil and the length of rod plays an important role for illustrating the structural phase transitions in rod-coil copolymers. In the symmetric configuration, the plate is a stable state. Otherwise, the spherical structure is a stable state for asymmetric configuration. The theoretical results answer the question of why the hollow structure can be formed and reveal its physics mechanism.

References

[1] Jenekhe S A and Chen X L 1998 *Science* **279** 1903
[2] Kresge C T, Leonowics M E, Woth W J, Vartuli J C and Beck J S 1992 *Nature* **359** 710
[3] Hamley I W 1998 *The Physics of Block Copolymers* (Oxford: Oxford University Press)
[4] Thurn-Albrecht T, Schotter J, Kastle G A, Emley N, Shibauchi T, Krasin-Elbaum I, Gaurini K, Black C T, Tuominen M T and Russell T P 2000 *Science* **290** 2126
[5] Segalman R A, McCulloch B, Kirmayer S and Urban J J 2009 *Macromolecules* **42** 9205
[6] Kato T, Mizoshita N and Kishimoto K 2006 *Angew. Chem. Int. Ed.* **45** 38
[7] Ries G 2003 *Prog. Polym. Sci.* **28** 1107
[8] Zhang L and Eisenberg A 1996 *J. Am. Chem. Soc.* **118** 3168
[9] Jain S and Bates F S 2003 *Science* **300** 460
[10] Wang C Y and Lodge T P 2002 *Macromolecules* **35** 841
[11] Zhang L and Wang P Y 2011 *Eur. Phys. J. E* **34** 43
[12] Geng X B, Pan J X, Zhang J J, Sun M N and Cen J Y 2018 *Chin. Phys. B* **27** 058102
[13] Jenekhe S A and Chen X L 1999 *Science* **283** 372
[14] Semenov A N 1985 *Sov. Phys. JETP* **61** 733
[15] Shi A C, Noolandi J and Hoffmann H 1994 *Macromolecules* **27** 6661
[16] Zhang Q Y and Xiang X 2013 *Chin. Phys. B* **22** 038201
[17] Boal D 2001 *Mechanics of the Cell* (Cambridge: Cambridge University Press)
[18] Zeng J B, Li L J, Liao Q, Chen Q H, Cui W Z and Pan L M 2010 *Acta Phys. Sin.* **59** 178 (in Chinese)
[19] Zhang L, Wang P Y and Shi A C 2009 *Sci. Chin. G* **39** 518